Solvent-Free Hydrogenation of Squalene Using Parts per Million Levels of Palladium Supported on Carbon Nanotubes: Shift from Batch Reactor to Continuous-Flow System

Boris Guicheret,[a, b] Laurent Vanoye,[a] Camila Rivera-Cárcamo,[c, d] Claude de Bellefon,[a] Philippe Serp,[c] Régis Philippe,*[a] and Alain Favre-Réguillon*[a, e]

The transition from batch catalytic processes to continuous flow processes requires highly active and stable catalysts that still need to be developed. The preparation and characterization of catalysts where palladium single atoms and nanoparticles are simultaneously present on carbon nanotubes were recently reported by us. These catalysts are considerably more active than commercial or previously described catalysts for the liquid phase hydrogenation of terpenes. Herein is shown that under solvent-free conditions, squalene (SQE) could be converted into squalane (SQA, > 98 %) using only 300 ppm of Pd in less than 1.4 h at 20 bar H_2 and 120 °C. Catalyst stability was assessed in a lab-scale flow reactor, and long-term experiments led to turnover number (TON) higher than 300000 without any detectable loss in the activity. Then, the implementation of this catalyst in a commercial intensified continuous-flow milli-reactor pilot was achieved. High purity SQA (> 98 %) could be obtained by continuous hydrogenation of solvent-free SQE at 180 °C and 30 bar H_2 with a contact time below 15 min. A production capacity of 3.6 kg per day of SQA could be obtained with an effective reactor volume (V_R) of 43.2 mL for this complex 3 phase reaction. Large-scale production can now be foreseen thanks to seamless scale-up provided by the continuous flow pilot supplier.

Introduction

The most challenging problem currently facing the pharmaceutical and specialty chemical industries is the transformation of existing batch catalytic processes into continuous flow processes. Such transformation promises many benefits, such as increased safety, simpler scale-up, access to novel processing windows, and higher throughput. The transition would be easier if highly active and stable catalysts are developed. In addition, from a green chemistry perspective, solvent-free chemical transformations are more interesting than reactions carried out with solvents.[1] However, from a process chemistry perspective, solvent-free reactions are linked to safety issues (for highly exothermic reactions), mass transfer limitation (for

viscous products), and inhibition (for bio-based substrates[2] and among them terpenes[3]). Therefore, the development of environmentally friendly solvent-free reactions continues to be of great concern.

The reduction of squalene (SQE) into squalane (SQA) is a representative illustration of this particular challenge (Figure 1). SQE is a linear triterpene present in the cells of all living organisms, which is extensively used in pharmaceuticals, food supplements, and cosmetics due to its multiple functions.[4] The global SQE market size was higher than USD 110 million in 2016 and is expected to witness significant growth over the following years.[4] In order to increase its stability (SQE oxidizes quickly due to its unsaturated character), SQE could be fully hydrogenated to SQA (Figure 1). Besides applications in

[a] Dr. B. Guicheret, Dr. L. Vanoye, Dr. C. de Bellefon, Dr. R. Philippe, Dr. A. Favre-Réguillon
Catalyse Polymérisation Procédés & Matériaux (CP2M)
Université Lyon
UMR 5128 CNRS – CPE Lyon, 43 boulevard du 11 novembre 1918,
F-69100 Villeurbanne (France)
E-mail: regis.philippe@lgpc.cpe.fr
[b] Dr. B. Guicheret
Present address:
Activation
10 rue Jacquard, 69680 Chassieu (France)
[c] Dr. C. Rivera-Cárcamo, Prof. P. Serp
ENSIACET
Université de Toulouse
LCC CNRS-UPR 8241, F-31030 Toulouse
(France)
[d] Dr. C. Rivera-Cárcamo
Present address:
ICPEES UMR 7515 CNRS
25 rue Becquerel, 67087 Strasbourg cedex 02
(France)
[e] Dr. A. Favre-Réguillon
Département Chimie-Vivant-Santé
Conservatoire National des Arts et Métiers
292 rue Saint Martin, F-75003 Paris
(France)
E-mail: favroreg@cnam.fr

Supporting information for this article is available on the WWW under https://doi.org/10.1002/cssc.202200916

ChemSusChem

Research Article
doi.org/10.1002/cssc.202200916

**Chemistry
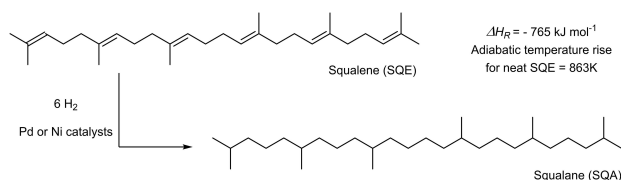Europe**

European Chemical
Societies Publishing

Figure 1. Hydrogenation of SQE into SQA.

cosmetics and pharmaceuticals, SQA, because of its high boiling point, inertness, low viscosity, and high gas solubility, is an interesting apolar solvent used as the reaction medium for catalytic tests[5] or the synthesis of quantum dots.[6]

The highly exothermic hydrogenation of SQE is traditionally carried out in stirred tank reactor using high loading of Ni- and Pd-based catalysts under harsh conditions and/or long reaction time (Table 1). Under those conditions, fast and irreversible catalyst deactivation and metal leaching occur, requiring product purification and catalyst refining and remanufacturing.[7] As such, purification by distillation could be necessary to obtain high-quality SQA, which increases overall production costs. Furthermore, safety issues arise due to the exothermicity of the reduction ($\Delta H_R = -765 \, kJ \, mol^{-1}$). An adiabatic temperature rises higher than 860 K for the neat reduction of SQE could be calculated. Thus, intentionally suboptimal operation conditions for safety reasons are generally implemented at an industrial scale, i.e., a two-step, one-pot process. The first step is performed at low H_2 pressure to initiate the reduction without the risk of a thermal run-away, followed by a subsequent step at higher H_2 pressure and temperature to obtain the total reduction (Table 1, entries 1, 3, 4, and 7). At the lab scale, solvent-free SQE could be fully hydrogenated using new Pd-based catalysts, but prolonged reaction time and harsh conditions are still required (Table 1, entries 3, 4 and 5).

Nickel-based catalysts have been traditionally used for the hydrogenation process.[8] Ni-catalysts require higher metal loading and temperatures (Table 1, entries 7 to 10). From an economic point of view, the additional cost related to the lower activity of the Ni-based catalyst could be balanced by the abundance and cost of Ni compared to Pd. However, the main problem of Ni-based catalysts is catalyst deactivation[9] and leaching.[7] Reasons for this are mainly the sintering of nickel crystallites under hydrogen.[10] Thus, there is a strong requirement for more active and stable hydrogenation catalysts to convert SQE into SQA.

Recently, we prepared new Pd-supported catalysts on carbon nanotubes (CNT), bearing both Pd nanoparticles (Pd_{NP}) and Pd single atoms (Pd_{SA}).[16] We demonstrated that the control of the ratio between Pd_{SA} and Pd_{NP} on carbon supports enables, thanks to cooperative catalysis,[17] the development of very active hydrogenation catalysts integrating the ultra-rational usage of precious metals.[18] In particular, we reported that Pd/CNT catalysts show high activity compared to catalysts already described for hydrogenation of terpenes, i.e., myrcene and SQE in solution (0.33 M in heptane).[18b] These catalysts should meet the need to increase catalytic activity for a highly demanding reaction like solvent-free hydrogenation of SQE (Table 1, entry 6).

Herein, we compared the Pd/CNT catalyst activity with commercial catalysts and evaluated the Pd/CNT catalyst stability in continuous flow reactors after its immobilization on a metallic foam. Then, a commercial pilot-scale continuous flow reactor was implemented to demonstrate its efficiency and robustness to provide a safe, compact, intensified, and scalable production process developed for the solvent-free hydrogenation of SQE.

Results and Discussion

Solvent-free hydrogenation of SQE with commercial catalysts

The solvent-free reduction of SQE was first studied using commercial catalysts as a benchmark. The reaction progress could not be easily followed by in situ or ex situ analysis. SQE has 6 double bonds with similar reactivity (all tri-substituted double bonds), and partial reduction leads to the formation of many isomers and diastereoisomers (there are 4 prochiral carbon in SQE). Nevertheless, reactant (SQE) and product (SQA) could be identified and quantified from the bulk of intermediates using GC/FID (Gas Chromatography with Flame Ionization Detection) with tetradecane as an internal standard (Figure 2).

Table 1. Experimental conditions for solvent-free hydrogenation of SQE.

Entry	Catalysts	Metal loading	Reaction conditions [temp. – P H₂]	Time [h]	Ref.
1	Pd/clay	1 mol%	300 °C[a] – 10 bar[b]	10	[3a]
2	Pd/organosilica	0.2 mol%	70 °C – 3 bar	24	[3b]
3	Pd/C	0.1 mol%	120 °C – 50 bar then 160 °C – 150 bar	[c]	[11]
4	Pd/C	0.1 mol%	25 °C – 65 bar then 60 °C – 65 bar	47	[12]
5	Pd/γ-Al₂O₃	0.08 mol%	120 °C – 20 bar	8.6	this work
6	Pd/CNT	0.03 mol%	120 °C – 20 bar	1.4	this work
7	Ni/diatomaceous earth	0.5 wt%	120 °C – 50 bar then 280 °C – 50 bar[d]	5	[13]
8	W6 Raney Ni	2.3 wt%	170 °C – 10 bar	3	[14]
9	Ni/kieselguhr	0.05 wt%	200 °C – 4 bar	3	[15]
10	Ni/SiO₂—Al₂O₃	2 mol%	150 °C – 20 bar	5	this work

[a] Temperature was gradually increased from 25 °C at a rate of 5 °C min⁻¹. [b] H₂ pressure at 25 °C. [c] Not provided. The reaction was stopped when H₂ uptake ceased. [d] H₂ was purged before heating to 280 °C.
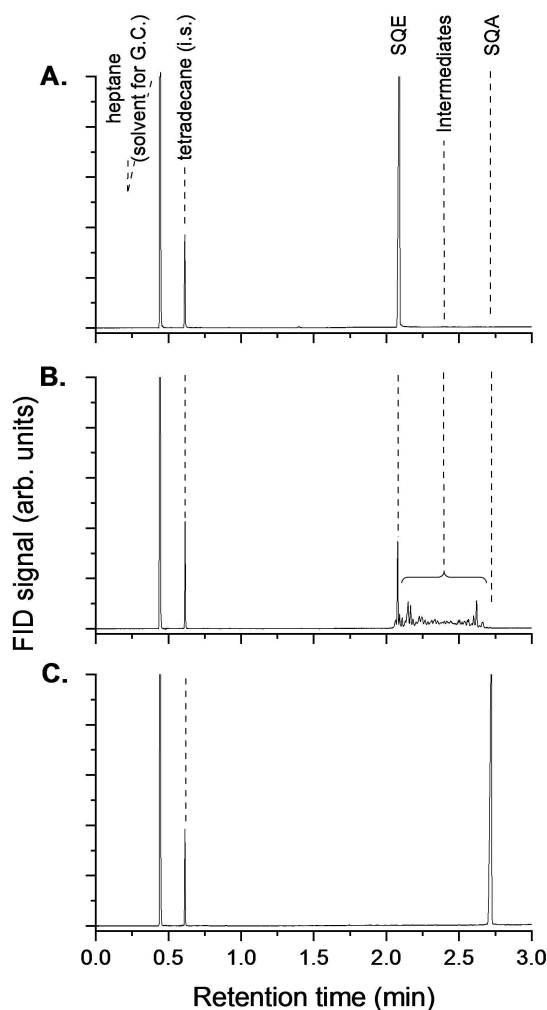
Figure 2. Comparison of the GC/FID chromatograms as the function of reaction progress. (A) Initial composition of the reaction mixture. (B) Reaction mixture at 85% conversion, 1 h. (C) Final composition of the reaction mixture after 9 h (conversion > 98%). Reaction conditions: H_2 20 bar; 120 °C; liquid phase 80 mL of solvent-free SQE (2.03 M) with tetradecane as internal standard (0.1 M); Pd 0.08 mol% (280 mg of 5 wt. % Pd/γ-Al$_2$O$_3$), 120 °C. Heptane was used to dilute the reaction mixture for GC analysis. (See Supporting Information in Figures S1 to S4 for full-scale chromatograms).

Figure 3. H_2 consumption and temperature of the liquid phase as the function of time. Reaction conditions: H_2 20 bar; 120 °C; liquid phase 80 mL of solvent-free SQE (2.03 M) with tetradecane as internal standard (0.1 M); (A) Pd 0.08 mol% (280 mg of 5 wt% Pd/γ-Al$_2$O$_3$), 120 °C; (B) Ni 2 mol% (300 mg of 65 wt% Ni/SiO$_2$-Al$_2$O$_3$), 120 °C for 0.5 h then 150 °C.

Furthermore, monitoring H_2 consumption as the function of time (Figure 3), associated with off-line GC/FID analysis, could give highly reproducible monitoring of the catalyst activity.

By using commercial 5 wt% Pd/γ-Al$_2$O$_3$, under typical conditions (120 °C, H_2 20 bar, 2 mol% Pd), the solvent-free catalytic reduction of SQE was achieved after 8.6 h (Figure 3a). The time required to achieve the total transformation of SQE into SQA is comparable to published data (Table 1). For SQE hydrogenation in heptane (0.33 M), complete saturation was obtained in less than 0.3 h for equivalent experimental conditions (Figures S5 and S6). The strong adsorption of SQE could explain this concentration effect and partially hydrogenated products on the catalyst surface, resulting kinetically in a term of inhibition by the reactant on the Langmuir-Hinshelwood-Hoogen-Watson (LHHW) rate law.[3a,19] The reduction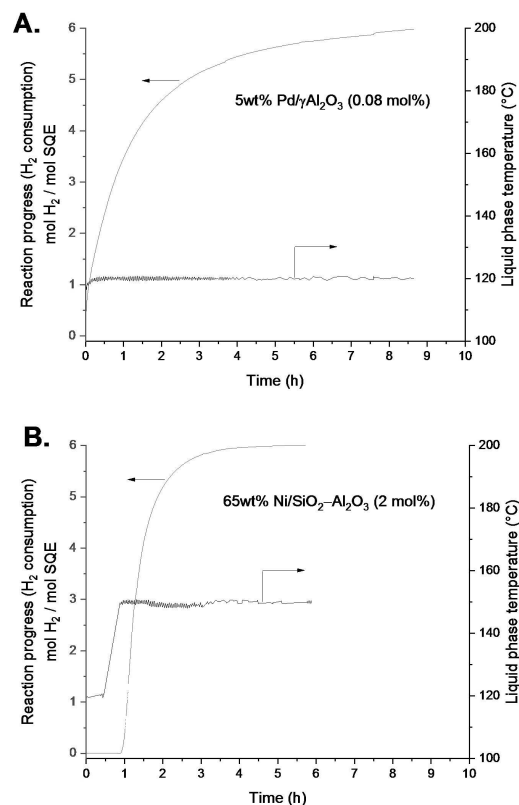 of solvent-free SQE was also studied with 2 mol% Ni using a commercial 65 wt% Ni/SiO$_2$-Al$_2$O$_3$ catalyst under the same conditions (Figure 3b). After 30 min at 120 °C, no H_2 consumption could be detected, and thus the reactor temperature was heated up to 150 °C. Then a slow reduction of the solvent-free SQE could be observed, and total reduction could be obtained after more than 5 h at 150 °C. Ni-based catalysts have been traditionally used for the hydrogenation process of SQE and other natural products.[8] From an economic point of view, the additional cost related to the lower activity of the Ni-based catalyst could be balanced by the abundance and cost of Ni compared to Pd. However, the main problem of this type of catalyst is catalyst deactivation[9] and Ni leaching.[7] Reasons for this are mainly the sintering of nickel crystallites under hydrogen.[10] Thus, there is a strong requirement for stable and highly active catalysts.

Solvent-free hydrogenation of SQE with Pd/CNT

Our group recently reported that Pd supported on mesoporous nano-carbon catalysts showed high activity for the hydrogenation of terpenes in heptane (β-myrcene, SQE)[16,18] and demonstrated that Pd$_{SA}$ and Pd$_{NP}$ were simultaneously present on the carbon supports. Unique cooperative catalysis operates

ChemSusChem

Research Article
doi.org/10.1002/cssc.202200916

Chemistry Europe
European Chemical
Societies Publishing

between these species, allowing one to reach very high activity for alkene hydrogenation through an H-spillover assisted mechanism involving the support functionalized surface.[18a,20] On CNT support, the optimum Pd_{SA}/Pd_{NP} ratio was found at 10/1 for terpene hydrogenation in solution.[18] The main characteristics of the Pd/CNT catalyst used for SQE hydrogenation are summarized in the Experimental Section (other characterizations can be found in Ref. [18a]), and Figure 4 shows representative high-angle annular dark-field scanning transmission electron microscopy (HAADF-STEM) micrographs (Pd_{SA} are circled in yellow for better visualization).

It has been previously shown that the activities of such Pd/CNT catalysts are very high.[18] For safety reasons, the amount of Pd was thus decreased to 0.03 mol% (300 ppm). The solvent-free reduction of SQE was first studied under standard conditions, i.e., 120°C, 20 bar H_2 (Figure 5).
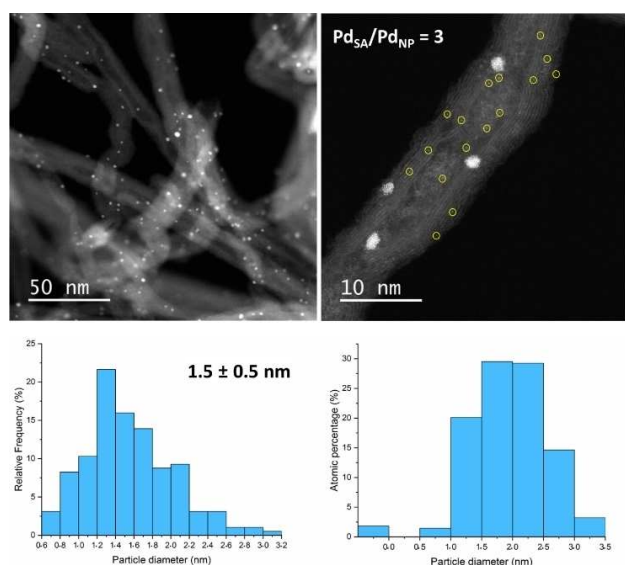

Figure 4. HAADF-STEM micrographs and particle size distribution are based on total particles and total atoms for Pd/CNT catalyst.
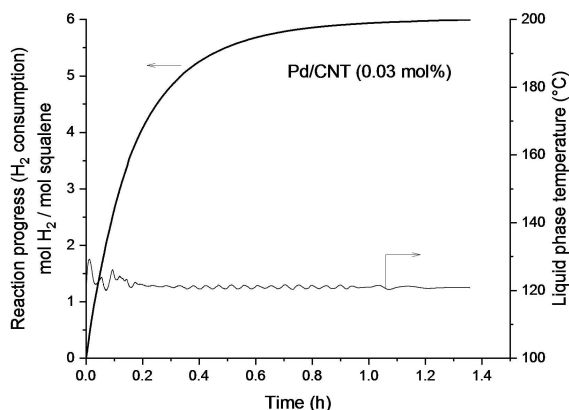

Figure 5. H_2 consumption and temperature as the function of time. Reaction conditions: H_2 20 bar; 120°C; liquid phase 80 mL of solvent-free SQE (2.03 M) with tetradecane as internal standard (0.1 M); Pd 0.03 mol% – 300 ppm (270 mg of 2.04 wt% Pd/CNT).

Under those conditions, the total and selective reduction of SQE into SQA was achieved in less than 1.4 h with 300 ppm of Pd (Table 1, entry 6). Despite using an efficient Ranque-Hilsch vortex device for cooling the relatively small stirred tank reactor (200 mL), the liquid phase temperature reaches 130°C within the first min of reaction. Such heat release obtained for 300 ppm of Pd prevents the use of higher catalyst loading in a batch reactor. However, this result clearly demonstrates that Pd supported on CNT that combines Pd_{SA} and Pd_{NP} can reach a very high activity for SQE hydrogenation under solvent-free conditions. This catalyst is much more efficient than the catalysts already described in the literature (Table 1) for the solvent-free reduction of SQE. The implementation of this catalyst in a continuous flow reactor was performed to evaluate its stability. Furthermore, the use of an intensified reactor with efficient heat transfer will enable us to study new process windows for this reaction[21] and to propose a more intense/efficient reactor for heat transfer and thus be able to propose a synthesis with new operating conditions.

Assessment of catalyst stability

The catalyst's stability could be evaluated by several consecutive batch reactions under the same conditions. In each cycle, after completion of the reduction, the catalyst should be collected by filtration, washed, dried, and reused in a subsequent cycle. Under these conditions (Figure 5), a maximum turnover number (TON) of 20000 could be achieved for such a cycle.

Otherwise, implementing this catalyst in a continuous flow reactor is an outstanding approach to demonstrate heterogeneous catalyst's stability with access to very high TON. However, implementing Pd/CNT catalyst in a continuous flow microreactor is not straightforward since Pd/CNT is a nano-textured micro powder (particle size < 10 μm). Heterogeneously catalyzed reactions with powder catalysts typically used in stirred tank reactors (particle size between 10–100 μm) have been successfully used in microreactors.[22] The catalysts could be confined in micro-packed bed systems,[23] but limitations such as high-pressure drops and possible temperature gradients are likely. This is especially relevant with the viscous SQE/SQA charge (36.1 and 2.2 mPa s^{-1} for SQA at 20°C and 120°C compared to 0.39 mPa s^{-1} for heptane at 20°C).[24] New strategies, adapted explicitly to micro- or milli-reactors, have been developed, such as catalytic static mixers (CSM),[25] and metallic open cell foams (OCF).[26] These scaffolds, coated with an active porous catalyst layer, can be inserted into continuous flow reactors. CSM should be specifically designed to fit the microreactors and could be produced by additive manufacturing.[27] Another approach would be to use high voidage structured materials commercially available at low cost, i.e., OCF. With their excellent thermal performance and large external specific surface area (up to 10000 m^2 m^{-3}), OCF have demonstrated their importance as heat exchangers, internal mixers, and catalyst supports.[26,28]

Fecralloy metallic foams (Hollomet, Foamet 400 μm, void fraction 92%, and geometrical specific surface area of 7000 m^2 m^{-3}) could be precisely adapted as milli-reactors internals from a foam sheet by electro-machining discharge. This offers a good cutting accuracy (± 5 μm) for conductive substrates, ensuring adaptability to various reactor geometries and intimate contact with channel walls, avoiding by-pass flows. OCF millimeter-scale blocks were then dip-coated with an aqueous suspension of the Pd/CNT catalyst (100 g L^{-1}) according to a reported procedure.[29] A final heat treatment at 300 °C under a reductive N$_2$-H$_2$ mixture provides the final supported catalyst. The coated OCF were controlled by optical microscopy (Figure S7) and elemental analysis. A mean catalyst content of 16.5 $\pm$ 5.0 g Pd/CNT catalyst per L of foam was obtained. The coating process did not significantly modify the particle size distribution (2 $\pm$ 0.5 nm) and the Pd$_{SA}$/Pd$_{NP}$ ratio (5.6) of the Pd/CNT catalyst (Figure S8), pointing to its high thermal stability.

The coated OCF were inserted into a homemade millimeter-scale tubular reactor (4 tubes of 100 mm length and 4.4 mm internal diameter) to provide an effective reactor volume (V_R) of 5.8 mL with a total catalyst amount of 0.1 g. These tubes are positioned in series in a thermoregulated oven (Figure 6), and thermocouples are distributed along the tube allow for measuring the axial temperature profile (See Supporting Information for details).

The continuous experiments were performed at 180 °C and 30 bar of H$_2$ with solvent-free SQE (2.03 M) to obtain a total reduction of SQE. An H$_2$/SQE molar ratio higher than 14 was used to ensure a large excess of H$_2$. First, the influence of contact time, defined as the ratio between the effective reactor volume (V_R) and the liquid flow (Q_L), on the yield in SQA and conversion of SQE was studied in this configuration. The results are shown in Figure 7.

For a contact time below 6 min at 180 °C and 30 bar H$_2$, total conversion of SQE was obtained, and the yield in SQA was up to 70% (Figure 7). These results further emphasized the synergy between the high activity of the Pd/CNT catalyst and the mixing effect of the metallic foam on H$_2$ mass transfer. No increase in the liquid phase temperature inside the reactor
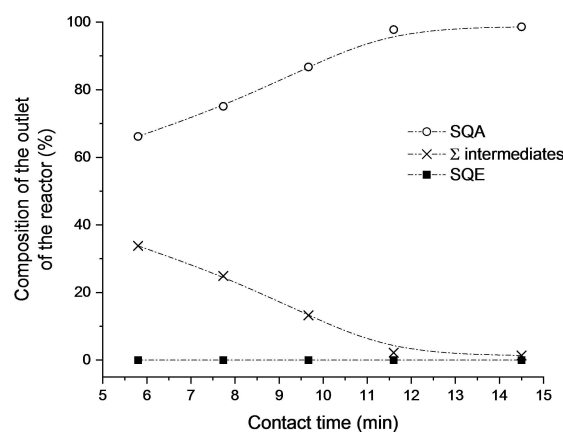
Figure 7. Composition at the outlet of the reactor as the function of contact time. Reaction conditions: effective reactor volume (V_R) 5.8 mL; 95.7 mg of 2.04 wt% of Pd/CNT coated on Fecralloy OCF (Foamet 400 μm); solvent-free SQE (2.03 M) with tetradecane as internal standard (0.1 M); 180 °C; H$_2$ 30 bar; ($Q_G/Q_L)_0 > 30$. SQA and SQE concentrations were determined by GC/FID using internal calibration. The concentration of the different intermediates was calculated by the difference in the concentration of SQA and SQE (see text and Figure 2). Lines are guides to the eyes.

could be noticed. In order to increase the yield in SQA, the contact time was increased by decreasing the liquid flow (Q_L). For a contact time higher than 14 min, at 180 °C and 30 bar of H$_2$, the yield of SQA was higher than 98%.

Figure 8 depicts two distinct parameters to illustrate the long life and the stability along time on stream of the studied catalytic system. The first one (squares) reflects the entire catalyst work through the evolution of the TON as the function of time on stream during the continuous hydrogenation of SQE. It should be mentioned that the TON* used [Figure 8, Eq. (1)] is largely minimized compared to the TON value since only the amount of SQA produced was considered as part of calculation. Intermediates, i.e., partially hydrogenated SQE, should theoretically be considered for the TON's determination. However, since they could not be precisely quantified (Figure 2), the TON* calculation was only based on the SQA produced [Eq. (1)].
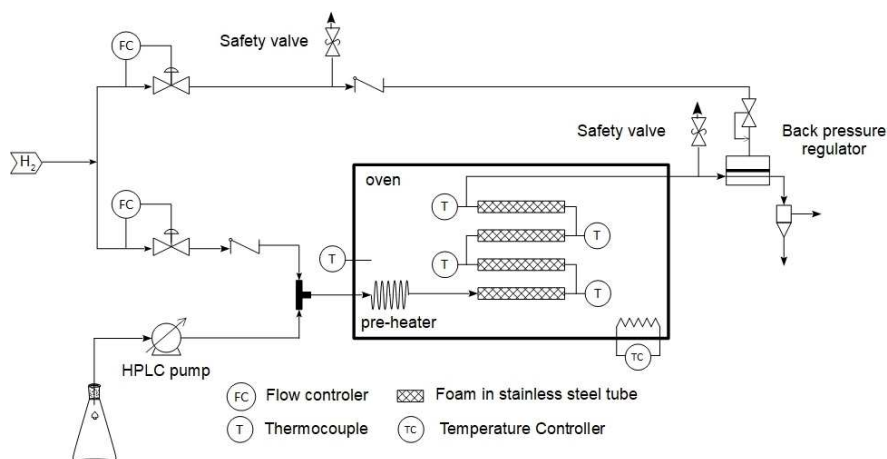
Figure 6. Experimental setup for the assessment of Pd/CNT catalytic stability.

ChemSusChem

Research Article
doi.org/10.1002/cssc.202200916

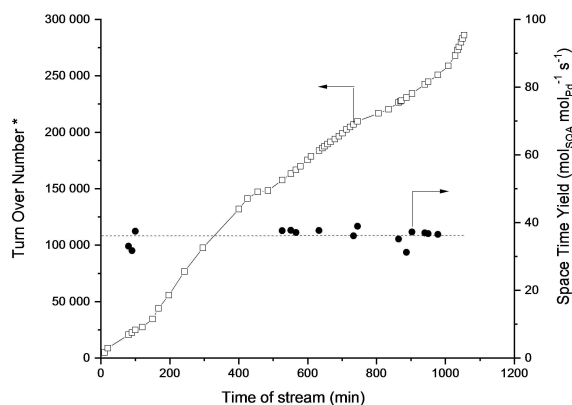**Chemistry Europe**
European Chemical
Societies Publishing

Figure 8. TON* and STY as the function of time on stream. TON* (squares) was determined according to Equation (1); intermediates were not considerate (see text). STY (blacked circles) was determined according to Equation (2) for reference recurrent experimental conditions (see text). Reaction conditions: effective reactor volume (V_R) 5.8 mL; 95.7 mg of 2.04 wt % of Pd/CNT coated on Fecralloy OCF (Foamet 400 μm); H_2 30 bar; SQE concentration between 0.33 and 2.03 M (solvent-free) with tetradecane as internal standard (0.1 M); temperature between 120 and 180 °C; Q_G between 0.16 and 1.2 nL/min⁻¹; Q_L between 0.4 and 8 mL min⁻¹. Lines are guides to the eyes. See Supporting Information in Figure S10 for details.

$$TON^* = \frac{6 \times \text{mol of SQA produced}}{\text{mol of Pd}} \qquad (1)$$

It is to be mentioned that these TON* are obtained under various experimental conditions, i.e., different temperatures, gas and liquid flow, and different concentrations of SQE, explaining the variations in the slope of the TON* as the function of time on stream. Under those conditions, a TON* up to 300000 mol_{H2}/mol_{Pd} could be determined (Figure 8).

The second parameter (black circles) is dedicated to periodic control experiments of the space-time yield (STY). STY measures the catalytic activity of the supported catalyst [Eq. (2)] under rigorously identical experimental conditions (i.e., SQE 0.3 M in heptane, contact time 2.9 min, 120 °C, and 30 bar of H_2).

$$STY = \frac{\text{mol of SQA produced per second}}{\text{mol of Pd}} \qquad (2)$$

Determinations of STY were performed regularly (Figure 8), and a mean value of 36 ± 5 mol_{SQA} mol_{Pd}^{-1} s^{-1} for STY was obtained throughout the experiment. No decrease of the STY as the function of time on stream could be noticed for a time on stream higher than 18 h (Figure 8). A stable STY value [Eq. (2)] could be determined even after different flow experiments in the vast experimental domain investigated, highlighting the high stability of the supported catalyst.

Determination of residual Pd by inductively coupled plasma mass spectrometry (ICP-MS) in the product is a classic method to identify Pd leaching. However, we believe, using a continuous flow experiment (Figure 8), that we were able to demonstrate more convincingly that the amount of Pd which leached into the product (SQA) is low, below the detection limit of ICP-MS. Indeed, in the worst-case scenario, one could speculate that all the Pd coated on the OCF (i.e., 1.95 mg) leached and accumulated in the product (SQA). Using a TON* of 300000, a maximum theoretical concentration of 5 ppm of Pd in SQA could be obtained. Furthermore, based on the value of STY, no deactivation could be highlighted during the time-on-stream experiment.

Additionally, HAADF-STEM analyses carried out on the spent catalyst do not show any significant modification in the size of the palladium particles and the Pd_{SA}/Pd_{NP} ratio (Figures S8 and S9), pointing to its high thermochemical stability.

Scale-up and transposition to a commercial intensified pilot reactor

With highly efficient catalysts, demanding batch hydrogenation protocols create safety hazards, particularly when large-scale reactors are required, because of reduced heat transfer capacities compared to lab-scale. Furthermore, the resulting temperature excursions may affect the selectivity of the transformations and cause the deactivation of the catalysts. This is particularly significant in the case of solvent-free SQE hydrogenation, where an adiabatic temperature rise of 863 K could be estimated. These safety concerns associated with mass transfer-limited reaction kinetics hindered the further development of highly efficient hydrogenation catalysts in physically limited reactors.

Contrary to stirred tank batch reactors, heat exchange in structured micro-/milli-reactors is sufficiently intense that even highly exothermic reactions can be conducted under nearly isothermal conditions.[30] Furthermore, due to the large interfacial areas, very efficient hydrogen mass transfer is achieved.[31] Finally, continuous processes are inherently safer for a given production capacity because of drastically reduced reactor inventories in opposition to stirred tank batch reactors. For these reasons, continuous-flow hydrogenation protocols employing metal catalysts have increased significantly over the past few years.[22a,32]

In order to demonstrate the robustness and the scalability of the results obtained in the homemade laboratory reactor, a transposition of the solvent-free SQE hydrogenation to a commercial intensified reactor was studied. The Miprowa-Lab reactor from Ehrfeld Mikrotechnik[33] (Figure 9a) was chosen for its similar millimeter-range hydraulic diameter (12×1.5 mm²) and its possible and easy operation with coated foam internals (Figure 9b). This reactor presents a practical reacting volume of 43.2 mL (divided into 8 channels in series), corresponding to a potential scale-up factor of 7.5 compared to our homemade tubular reactor (5.8 mL). Again, foam pieces were precisely cut in the same foam block to be mounted inside the 8 channels after coating with the same Pd/CNT catalyst (Figure 9c). A catalyst content of 16.5 ± 4.0 g of Pd/CNT catalyst per L of foam was obtained, close to the one obtained for the tubular reactor.

Table 2 compares the two reactors for two different contact times, i.e., 14.4 min and 9.6 min, under the same experimental conditions (180 °C, 30 bar H_2, solvent-free SQE). For a given

ChemSusChem

Research Article
doi.org/10.1002/cssc.202200916

Chemistry Europe
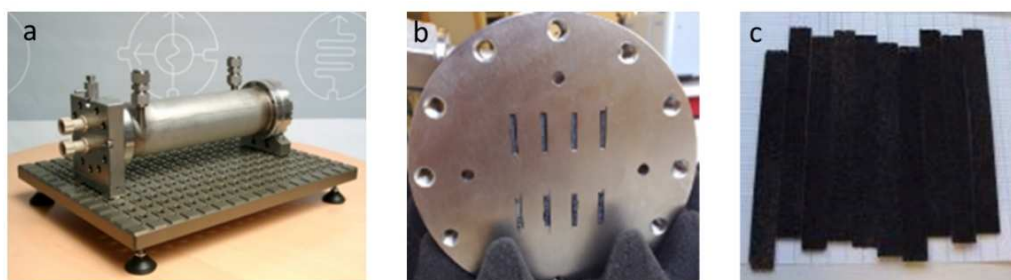European Chemical
Societies Publishing

Figure 9. (a) Ehrfeld Mikrotechnik Miprowa-Lab reactor. (b) Head of the reacting zone showing the foam sheets internals. (c) Coated foam sheets with Pd/CNT catalyst.

Table 2. Comparison of a homemade tubular reactor ($V_R = 5.8$ mL) and commercial intensified reactor ($V_R = 43.2$ mL) at two operating points.[a]

Effect [mL]	Contact time [min]	Q_L [mL min^{-1}]	SQA yield[b] [%]	STY [mol$_{SQA}$ mol$_{Pd}^{-1}$ min^{-1}]	SQA production capacity[c] [kg$_{SQA}$ day^{-1}]
Tubular	9.63	0.6	79.3	50.5	
(5.8)	14.45	0.4	>98.0	41.6	0.485
Miprowa-Lab	9.60	4.5	78.2	49.3	
(43.2)	14.40	3	>98.0	43.7	3.630

[a] Reaction conditions: solvent-free SQE (2.03 M) with tetradecane as internal standard (0.1 M); 180 °C; H$_2$ 30 bar; Pd/CNT coated on Fecralloy metallic foams (Foamet 400 μm). Catalyst content of 17.2 g and 16.5 g of Pd/CNT per L of foam for tubular and Miprowa-Lab reactor, respectively. $Q_G = 400$ NmL/min^{-1} and 3000 NmL/min^{-1} for tubular and Miprowa-Lab reactors, respectively. [b] SQA yield was determined by GC/FID using internal calibration. [c] SQA purity was higher than 98 % and could be used without further purification.

contact time, the SQA yields in different reactors are close, demonstrating the scalability of the coated foam contacting mode to a commercial reactor. A slight difference could be noticed, reflecting both the slight difference in catalyst content and possible variations in heat and mass transfer capacities due to the changes in the geometrical configuration of the reacting volume (channel section, channel length, aspect ratio, etc.) and wall heat exchanging system.

Transposition of SQE reduction at two similar operating points, from the homemade tubular reactor to the commercial intensified reactor, results in higher production capacity (Table 2). From lab-scale tubular reactor to Miprowa-Lab reactor, the production capacity of high purity SQA (>98 %) was increased by a factor of 7.5, i.e., 0.485 kg$_{SQA}$ per day to 3.630 kg$_{SQA}$ per day for tubular reactor and Miprowa-Lab reactor, respectively. Under these conditions, even if all Pd present in the microreactor was leached in 24 h, the amount of Pd present in SQA will be less than 50 ppb, far below the parenteral concentration limit for Pd in drug products, i.e., 1 ppm (1 μg g^{-1}) due to the toxicity of Pd (ICH classification 2b).[34] It should be noticed that the absence of appreciable deactivation during the 18 h time on stream study (Figure 8) indicates that the situation concerning Pd leaching is far from this most pessimistic scenario.

In case of coated foam availability, further seamless scale-up would be quickly and easily ensured (by the technology provider) up to reactor units able to process several m³ h^{-1}.[33] Other internals could also be coated, such as the pristine static mixing elements of Ehrfeld microreactors or CSM.[25b,27b] Before such demonstrations, identical transfer features need to be demonstrated, and the Pd/CNT catalyst coating has to be adapted. Furthermore, except for the first double bond hydrogenation of SQE, the reactor operates roughly in a chemical regime. Further process intensification can be expected thanks to this equipment with higher H$_2$ pressure and a slightly higher temperature operating window, which still needs to be investigated.

Conclusion

The catalytic activity of palladium catalyst with Pd single atoms (Pd$_{SA}$) and Pd nanoparticles (Pd$_{NP}$) supported on carbon nanotubes (CNT) was tested on solvent-free squalene's hydrogenation. The catalytic activity of Pd/CNT showed a tremendous improvement compared to previously described and/or commercially available catalysts. The total reduction of solvent-free squalene (SQE) into squalane (SQA) was effective at 120 °C, 30 bar H$_2$ using 300 ppm of Pd in less than 1.4 h in a lab-scale batch stirred tank reactor. The catalyst stability was assessed in a continuous flow reactor, and a turnover number (TON) higher than 300000 without any detectable loss in activity was demonstrated. A successful batch to a commercial continuous milli-structured pilot-scale reactor was then validated. These experiments assess the operability of such a catalyst in flow and its stability. Neat SQA (≥ 98 %) could be obtained continuously at 180 °C and 30 bar H$_2$ with a contact time below 15 min. Under those conditions, a space-time yield of 43.7 mol$_{SQA}$ mol$_{Pd}^{-1}$ min^{-1} and a high purity SQA production capacity of 3.6 kg per day was obtained using a commercial intensified reactor with an effective reactor volume (V_R) of 43.2 mL.

Experimental Section

Squalene and solvents

SQE (98%) was purchased from Aldrich and used as received. SQE was stored under refrigeration (2–8 °C) and protected from light. Heptane, EtOH, Triton X-100, and dextrin were purchased from Aldrich or Acros and used as received.

Catalysts

Pd^0/Al_2O_3 (Alfa Aesar, Product number 11713) and Ni/SiO_2-Al_2O_3 (Alfa Aesar, Product number 31276) were used directly without further treatment. Pd/CNT was prepared by wet impregnation method according to P. Serp and coworkers.[16] The main characteristics of these catalysts are summarized in Table 3, and Figure 4 shows representative HAADF-STEM.

Characterization of the catalysts

The palladium content in the products was measured by inductively coupled plasma optical emission spectroscopy (ICP-OES). Transmission electron microscopy (TEM) and high-resolution TEM (HR-TEM) analyses were performed at the "Centre de microcaracterisation Raimond Castaing, UMS 3623, Toulouse" by using a JEOL JEM 2100F equipped with a field emission gun (FEG) operating at 200 kV with a point resolution of 2.3 Å and a JEOL JEM-ARM200F Cold FEG operating at 200 kV with a point resolution of > 1.9 Å. The particle size distribution was determined by manually measuring enlarged micrographs from different areas of the TEM grid (at least 300 particles). The size distribution reported as Pd atomic percentage (based on total atoms) in each size range was obtained by calculating the number of atoms (N) in each nanoparticle, assuming a spherical shape using an equation described by A. Karim et al. .[37] The SA/NP ratio (a number ratio) was measured from the HAADF-STEM analyses of at least 500 elements. Optical microscopy was performed using optical microscope KEYENCE VHX 6000.

General procedure for the hydrogenation of SQE in a stirred tank reactor

The reaction was performed in a 200 mL thermo-regulated stainless steel autoclave from Top Industrie. A stainless steel insert with four baffles was mounted on the reactor walls, and the reaction medium was stirred by a gas-inducing Rushton impeller having six straight blades. Temperature control is provided by both an electric shell (for heating) and a Ranque-Hilsch vortex device (for cooling). The reactor is operated in batch mode for the liquid and solid phases and semi-batch mode for the gas phase. Hydrogen was constantly fed via a pressure regulator and supplied by a calibrated reserve. The pressure and temperature monitoring of this reserve provide the hydrogen consumption rate. The liquid phase temperature,

monitored using J-type thermocouples, and the time-course of hydrogen consumption, monitored with a pressure transducer, were acquired and recorded online using Labview® at 1 Hz.

The catalyst and 80 mL of solvent-free SQE, with tetradecane (0.1 M) as an internal standard, were placed in the reactor. The reactor was purged three times with N_2 at room temperature, and the reactor was heated up to the desired temperature under stirring. When the desired temperature was reached, stirring was stopped. The N_2 atmosphere was replaced by the H_2, and the experiment was re-started by switching on the agitator, determining the t_0 of the reaction.

At the end of each experiment, the reaction mixture was analyzed after dilution with heptane using an Agilent 6890 GC-FID and a Shimadzu 2010 GC-MS (Gas Chromatography with Mass Spectrometry) system, both equipped with DB-17 columns. Unlike other terpenes, the reactivity of the double bonds in SQE is quasi-identical (all tri-substituted double bonds). As such, the identification of different isomers as the function of time by GC/FID and GC/MS methods is impractical. Nevertheless, reactant (SQE) and product (SQA) could be identified and quantified from the bulk of intermediates using GC/FID with tetradecane as the internal standard (Figure 2). In-line H_2 consumption associated with off-line GC/FID analysis could give highly reproducible catalyst activity monitoring.

Dip-coating procedure

Preparation of the suspension

In the tank of a planetary mill, 20 mL of water was added with 1.1 mL of Triton X-100 and stirred at 300 rpm for 3 min. 0.8 g of dextrin was added, and the mixture was ball-milled for 5 min at 300 rpm. 5 g of Pd/CNT was added, and the mixture was again ball-milled for 45 min at 500 rpm. The final suspension of the catalyst was collected with water to reach a final concentration of 100 g L^{-1}.

Activation of the supports

Fecralloy metallic foams (Hollomet, Foamet 400 µm) were cut into cylinder-shaped blocks (length-diameter: 50 mm–4.3 mm) or into sheets (length, width, thickness: 150 mm, 12 mm, 1.5 mm). The metallic foams were carefully washed in acetone in a sonication bath, dried, heated to 500 °C for 4 h under 500 NmL/min^{-1} airflow, and then cooled to room temperature.

Dip-coating of the support

Activated substrates were dipped entirely in the catalyst suspension. Excess catalyst suspension was removed by airflow. The coated foams were dried under air at 80 °C overnight, then heated to 300 °C for 2 h under nitrogen/hydrogen flow (80/20) (total

Table 3. Catalysts' main characteristics.

Catalyst	Pd content [wt%]	BET surf. area [$m^2 g^{-1}$]	Particle size[a] [nm]	Pd dispersion[b] [%]	Pd_{SA}/Pd_{NP} ratio[c]
Pd/Al_2O_3[d]	5.00	140	n.d.	16	–
Ni/SiO_2–Al_2O_3	65	n.d.	n.d.	n.d.	–
Pd/CNT[e]	2.04	232	1.5 ± 0.5	67	3.1

[a] From TEM image. [b] Metal dispersion was evaluated from a universal mathematical relation between the mean relative size of metallic crystallites and their dispersion, as described elsewhere Ref. [35]. [c] The SA/NP ratio is a number ratio measured from the HAADF-STEM analyses. [d] See Ref. [36]. [e] See Ref. [16,18a].

ChemSusChem

Research Article
doi.org/10.1002/cssc.202200916

Chemistry
Europe
European Chemical
Societies Publishing

flowrate of 500 NmL/min^{-1}) and kept for 2 h at 300 °C. The oven was cooled to room temperature under nitrogen flow (500 mL min^{-1}). The amount of catalyst coated on the metallic foams was determined by weighing. Analysis of the Pd/CNT catalyst after coating shows that the coating process did not significantly modify the particle size distribution (2 ± 0.5 nm) and the Pd$_{SA}$/Pd$_{NP}$ ratio is 5.6 (Figure S8).

General procedure for the hydrogenation of SQE in flow in a milli-reactor

Coated foam pieces were inserted in a homemade milli-reactor (4 tubes in series of 100 mm length and 4.4 mm internal diameter) or in a Miprowa-Lab reactor (8 channels in series of 300 mm length with a width of 12 mm and a height of 1.5 mm). The temperature was controlled by a thermoregulated oven or a heated circulating bath (Figure 6 and Supporting Information). The temperature inside the reactor was monitored using J-type thermocouples.

In a 1000 mL volumetric flask, solvent-free SQE with tetradecane as internal standard (0.1 M), was prepared. At the reactor inlet, solvent-free SQE [ensured by a high-performance liquid chromatography (HPLC) pump Shimadzu LC 20 AD] and gas flow (regulated by a mass flow controller Bronkhorst Elflow Prestige) meet at a T junction. An Equilibar back pressure regulator precisely regulated outlet pressure. G—L separation and liquid collection are ensured by gravity. When a stable temperature was obtained, periodical analysis of the liquid phase by GC-FID and GC-MS after dilution with heptane was used to calculate the conversion of SQE and the yield of SQA.

Acknowledgements

Conflict of Interest

The authors declare no conflict of interest.

Data Availability Statement

The data that support the findings of this study are available from the corresponding author upon reasonable request.

Keywords: heterogeneous catalysis · hydrogenation · nanotubes · palladium · terpenoids

[1] a) Y. Jiang, R. Büchel, J. Huang, F. Krumeich, S. E. Pratsinis, A. Baiker, *ChemSusChem* **2012**, *5*, 1190–1194; b) T. Yu, J. Jiao, P. Song, W. Nie, C. Yi, Q. Zhang, P. Li, *ChemSusChem* **2020**, *13*, 2876–2893.

[2] a) J. Yang, N. Li, G. Li, W. Wang, A. Wang, X. Wang, Y. Cong, T. Zhang, *ChemSusChem* **2013**, *6*, 1149–1152; b) T. Wang, W. Xie, Y. Pang, W. Qiu, Y. Feng, X. Li, J. Wei, X. Tang, L. Lin, *ChemSusChem* **2022**, e202200186.

[3] a) V. K. Soni, R. K. Sharma, *ChemCatChem* **2016**, *8*, 1763–1768; b) V. Pandarus, R. Ciriminna, F. Beland, M. Pagliaro, S. Kaliaguine, *ACS Omega* **2017**, *2*, 3989–3996; c) A. Selka, N. A. Levesque, D. Foucher, O. Clarisse, F. Chemat, M. Touaibia, *Org. Process Res. Dev.* **2017**, *21*, 60–64; d) H. Fan, T. Zheng, X. Liao, M. Sun, J. Fu, J. Zheng, N. Zhang, B. Chen, *ChemCatChem* **2022**, *14*, e202101690.

[4] M. A. Lozano-Grande, S. Gorinstein, E. Espitia-Rangel, G. Dávila-Ortiz, A. L. Martínez-Ayala, *Int. J. Agron.* **2018**, Article ID 1829160. .

[5] a) A. García-Trenco, E. R. White, A. Regoutz, D. J. Payne, M. S. P. Shaffer, C. K. Williams, *ACS Catal.* **2017**, *7*, 1186–1196; b) C. Méhault, L. Vanoye, R. Philippe, C. de Bellefon, *Chem. Eng. J.* **2021**, *407*, 127215.

[6] D. C. Gary, M. W. Terban, S. J. L. Billinge, B. M. Cossairt, *Chem. Mater.* **2015**, *27*, 1432–1441.

[7] R. Ciriminna, V. Pandarus, F. Beland, M. Pagliaro, *Org. Process Res. Dev.* **2014**, *18*, 1110–1115.

[8] M. A. Stoffels, F. J. R. Klauck, T. Hamadi, F. Glorius, J. Leker, *Adv. Synth. Catal.* **2020**, *362*, 1258–1274.

[9] S. García, S. Poulston, P. Stavarek, in: *Industrial Green Chemistry* (Eds.: S. Kaliaguine, J.-L. Dubois), De Gruyter, **2020**, pp. 115–138.

[10] a) P. Birke, R. Geyer, M. Keck, A. Pachulski, R. Schödel, *Chem. Ing. Tech.* **2012**, *84*, 165–168; b) A. K. AlAsseel, S. D. Jackson, *Ind. Eng. Chem. Res.* **2021**, *60*, 15502–15513.

[11] K. Fisher, S. J. Schofer, D. Kane, **2011**, Amyris Biotechnologies, Inc., USA . Patent WO 2011/146837.

[12] K. Fisher, F. X. Woolard, **2010**, Amyris Biotechnologies, Inc., USA . Patent WO 2010/042208.

[13] K. Sogabe, T. Koshiyama, **2008**, New Japan Chemical Co., Ltd., Japan, Japan Patent N° 2008013477 (CAS Reaction Number: 31242-CAS-9507603).

[14] J. Dale, T. Artun, *Acta Chem. Scand.* **1956**, *10*, 439–444.

[15] C.-S. Wu, Y.-J. Tsay, H.-J. Liou, *J. Fish. Soc. Taiwan* **1980**, *7*, 43–55.

[16] R. C. Contreras, B. Guicheret, B. F. Machado, C. Rivera-Cárcamo, M. A. Curiel Alvarez, B. Valdez Salas, M. Ruttert, T. Placke, A. Favre-Réguillon, L. Vanoye, C. de Bellefon, R. Philippe, P. Serp, *J. Catal.* **2019**, *372*, 226–244.

[17] P. Serp, *Nanoscale* **2021**, *13*, 5985–6004.

[18] a) C. Rivera-Cárcamo, I. C. Gerber, I. del Rosal, B. Guicheret, R. Castro Contreras, L. Vanoye, A. Favre-Réguillon, B. F. Machado, J. Audevard, C. de Bellefon, R. Philippe, P. Serp, *Catal. Sci. Technol.* **2021**, *11*, 984–999; b) L. Vanoye, B. Guicheret, C. Rivera-Cárcamo, R. Castro Contreras, C. de Bellefon, V. Meille, P. Serp, R. Philippe, A. Favre-Réguillon, *Chem. Eng. J.* **2022**, *441*, 135951.

[19] V. Pandarus, R. Ciriminna, S. Kaliaguine, F. Beland, M. Pagliaro, *ChemCatChem* **2015**, *7*, 2071–2076.

[20] a) I. C. Gerber, P. Serp, *Chem. Rev.* **2020**, *120*, 1250–1349; b) J. Audevard, A. Benyounes, R. Castro Contreras, H. Abou Oualid, M. Kacimi, P. Serp, *ChemCatChem* **2022**, *14*, e202101783.

[21] V. Hessel, D. Kralisch, N. Kockmann, T. Noël, Q. Wang, *ChemSusChem* **2013**, *6*, 746–789.

[22] a) M. Irfan, T. N. Glasnov, C. O. Kappe, *ChemSusChem* **2011**, *4*, 300–316; b) R. Munirathinam, J. Huskens, W. Verboom, *Adv. Synth. Catal.* **2015**, *357*, 1093–1123; c) A. Tanimu, S. Jaenicke, K. Alhooshani, *Chem. Eng. J.* **2017**, *327*, 792–821.

[23] M. W. Losey, M. A. Schmidt, K. F. Jensen, *Ind. Eng. Chem. Res.* **2001**, *40*, 2555–2562.

[24] a) M. J. P. Comuñas, X. Paredes, F. M. Gaciño, J. Fernández, J. P. Bazile, C. Boned, J. L. Daridon, G. Galliero, J. Pauly, K. R. Harris, M. J. Assael, S. K. Mylona, *J. Phys. Chem. Ref. Data* **2013**, *42*, 033101; b) S. K. Mylona, M. J. Assael, M. J. P. Comuñas, X. Paredes, F. M. Gaciño, J. Fernández, J. P. Bazile, C. Boned, J. L. Daridon, G. Galliero, J. Pauly, K. R. Harris, *J. Phys. Chem. Ref. Data* **2014**, *43*, 013104.

[25] a) A. Avril, C. H. Hornung, A. Urban, D. Fraser, M. Horne, J. P. Veder, J. Tsanaktsidis, T. Rodopoulos, C. Henry, D. R. Gunasegaram, *React. Chem. Eng.* **2017**, *2*, 180–188; b) M. Kundra, T. Grall, D. Ng, Z. Xie, C. H. Hornung, *Ind. Eng. Chem. Res.* **2021**, *60*, 1989–2002.

[26] J.-N. Tourvieille, R. Philippe, C. de Bellefon, *Chem. Eng. J.* **2015**, *267*, 332–346.

[27] a) C. Parra-Cabrera, C. Achille, S. Kuhn, R. Ameloot, *Chem. Soc. Rev.* **2018**, *47*, 209–230; b) R. Lebl, Y. Zhu, D. Ng, C. H. Hornung, D. Cantillo, C. O. Kappe, *Catal. Today* **2022**, *383*, 55–63; c) G. Vilé, D. Ng, Z. Xie, I.

ChemSusChem

Research Article
doi.org/10.1002/cssc.202200916

Chemistry Europe
European Chemical
Societies Publishing

Martinez-Botella, J. Tsanaktsidis, C. H. Hornung, *ChemCatChem* **2022**, *14*, e202101941.

[28] J.-N. Tourvieille, R. Philippe, C. de Bellefon, *Chem. Eng. Sci.* **2015**, *126*, 406–426.

[29] F. Simescu-Lazar, T. Chaieb, S. Pallier, L. Veyre, R. Philippe, V. Meille, *Appl. Catal. A* **2015**, *508*, 45–51.

[30] H. P. Gemoets, Y. Su, M. Shang, V. Hessel, R. Luque, T. Noël, *Chem. Soc. Rev.* **2016**, *45*, 83–117.

[31] a) C. J. Mallia, I. R. Baxendale, *Org. Process Res. Dev.* **2015**, *20*, 327–360; b) C. A. Hone, C. O. Kappe, *Top. Curr. Chem.* **2018**, *377*, 2.

[32] a) V. Hessel, *Chem. Eng. Technol.* **2009**, *32*, 1655–1681; b) R. L. Hartman, J. P. McMullen, K. F. Jensen, *Angew. Chem. Int. Ed.* **2011**, *50*, 7502–7519; *Angew. Chem.* **2011**, *123*, 7642–7661; c) M. B. Plutschack, B. Pieber, K. Gilmore, P. H. Seeberger, *Chem. Rev.* **2017**, *117*, 11796–11893.

[33] Ehrfeld Mikrotechnik, Wendelsheim, Germany, https://ehrfeld.com/en/products/miprowar.html, (Accessed on 30 june 2022).

[34] In *ICH Harmonised Guideline, Guideline for Elemental Impurities, Q3D(R1) 22 March 2019, International Council For Harmonisation of Technical Requirements For Pharmaceuticals For Human Use*, https://www.ich.org/page/quality-guidelines (Accessed on 04 May 2022).

[35] A. Borodziński, M. Bonarowska, *Langmuir* **1997**, *13*, 5613–5620.

[36] A. Karelovic, P. Ruiz, *ACS Catal.* **2013**, *3*, 2799–2812.

[37] C.-T. Kuo, Y. Lu, L. Kovarik, M. Engelhard, A. M. Karim, *ACS Catal.* **2019**, *9*, 11030–11041.